Dynamic testing of post-tensioned rocking walls

K.M. Twigden, R.S. Henry & Q.T. Ma
Department of Civil and Environmental Engineering,University of Auckland, New Zealand

SUMMARY:
Post-tensioned precast concrete walls have been shown both experimentally and analytically to provide excellent seismic resilience. However, only a limited number of experimental tests have been conducted to investigate the dynamic response of such rocking wall systems. This paper presents the preliminary results of an experimental test program that was conducted to further understand the dynamic characteristics of post-tensioned rocking walls. The experimental test program investigated a single post-tensioned concrete wall subjected to pseudo-static cyclic loading, high speed cyclic loading, free vibration, and dynamic forced-vibration testing. The lateral load response was determined from both the pseudo-static and high speed cyclic tests, and closely matched the response calculated using an existing analysis procedure. Free vibration decay was used to determine the co-efficient of restitution which aligned well with Housner's formulation. The dynamic forced-vibration testing using an eccentric mass shaker excited the structure into the rocking mode and the lateral displacement response of the wall is presented.

Keywords: Unbonded post-tensioned; precast concrete; experimental dynamic testing; wall; rocking;

1. INTRODUCTION

Self-centering precast concrete structures that utilise unbonded post-tensioning have previously been shown both experimentally and analytically to demonstrate excellent seismic performance (Kurama et al., 1999a, Priestley et al., 1999). The use of precast concrete introduces dry connections that accommodate inelastic demand through opening and closing of an existing crack, introducing a rocking mechanism. The unbonded post-tensioning is designed to remain elastic during a design-level earthquake and provides a self-centering restoring force. The restoring force provided by the post-tensioning increases the stability of the rocking system against overturning. The combination of precast elements and unbonded post-tensioning generates a response that undergoes inelastic deformations with minimal damage. Post-tensioned precast concrete members have limited energy dissipation compared to a traditional reinforced concrete structure due to the minimal damage sustained from a seismic event.

The concept of self-centering precast concrete elements that utilise unbonded post-tensioning was investigated extensively during the Precast Seismic Structural Systems (PRESSS) research program conducted in the 1990's (Priestley, 1991). A jointed wall system that was developed during the PRESSS research program was included in the experimentally tested five storey prototype building (Nakaki et al., 1999, Priestley et al., 1999). Following the PRESSS research program several different rocking wall systems have been developed with a significant focus placed on the type and arrangement of additional energy dissipating elements (Holden et al., 2003, Restrepo and Rahman, 2007, Marriott et al., 2008, Kurama, 2000, Henry et al., 2010, Sritharan et al., 2007).

Unbonded post-tensioned rocking wall systems have been subject to numerous pseudo-static lateral load tests (Restrepo and Rahman, 2007, Perez et al., 2003, Perez et al., 2004, Holden et al., 2003,

Henry et al., 2012). Additionally, extensive analytical investigations have been performed which utilise nonlinear time history analysis to simulate the response of unbonded post-tensioned wall systems to earthquake excitation (Kurama et al., 1999b, Kurama et al., 2002, Erkmen and Schultz, 2009, Ma, 2010). However, only a limited number of experimental tests have been conducted to investigate the dynamic response of unbonded post-tensioned rocking wall systems. Understanding the dynamic behaviour of unbonded post-tensioned rocking wall systems is critical to assessing their seismic performance because dynamic characteristics can be neglected during pseudo-static testing. The damping in an unbonded post-tensioned system with no additional energy dissipating elements consists of contact damping and inherent Equivalent Viscous Damping (EVD). Contact damping is the energy loss due to the velocity reduction at impact during rocking (Ma, 2010). Contact damping is velocity dependant and therefore neglected during pseudo-static testing, this means contact damping can only be captured during true dynamic tests.

Dynamic testing of precast unbonded post-tensioned rocking walls has been limited to shake table testing carried out by Marriott et al. (2008) who conducted a total of 16 tests on four walls. Three of the tested walls had various types of additional energy dissipating elements and the fourth wall relied on contact damping and inherent EVD. Based on the experimental results, Marriott et al. quantified the contact damping between the wall and foundation to between 1-3% EVD. Additionally, the peak lateral displacements of the top of the wall were below the targets for the design level earthquake except for the wall with no additional energy dissipation. The inability to accurately design a wall with no additional energy dissipation highlights the current uncertainty with the evaluation of contact damping. Dynamic tests including shake table tests have also been carried out on post-tensioned masonry walls and post-tensioned bridge columns (Wight et al., 2006, Wight et al., 2007, Cheng, 2007, Cheng, 2008).

Unbonded post-tensioned rocking walls take advantage of a rocking mechanism. The majority of modern research on the mechanics of rocking objects stems from a paper by Housner (1963) on the behaviour of inverted pendulum structures during earthquakes. In this paper an expression for the apparent Coefficient Of Restitution (COR) was developed (Eq 1.1). The COR represents the ratio of kinetic energy immediately after, to that immediately before, an impact and can be used as a measure of contact damping in the form of the energy loss due to impacts.

$$COR = \left[1 - \frac{mR^2}{I_o}(1 - cos2\alpha)\right]^2 \tag{1.1}$$

Where m is the block mass, Io the moment of inertia, R the radial distance from the centre of rotation to the centre of gravity and α is the angle the rocking block makes while at rest between the vertical and R.

Ma (2010) investigated the apparent co-efficient of restitution of an unbonded post-tensioned masonry rocking wall. The energy content of the wall system was separated into three components, gravitational potential energy, kinetic energy, and elastic potential energy from the elongation of the prestressing tendon. The COR was calculated by obtaining the ratio of successive total energy content during free vibration decay.

2. EXPERIMENTAL TEST METHODOLOGY

An experimental study was conducted to investigate the cyclic and dynamic behaviour of unbonded post-tensioned rocking walls without additional energy dissipating elements. A single unbonded post-tensioned precast wall panel was subjected to a series of four different loading conditions, including pseudo-static cyclic loading, forced vibration loading, high-speed cyclic loading and snap-back free vibration testing.

2.1. Construction detail

The precast concrete wall test specimen was designed to be 3 m high, 1 m long and 0.12 m wide, as

shown in Figure 1. Because only minor damage was expected in the wall toes, the specimen had a symmetrical design to allow it to be flipped and retested on the other end. The post-tensioning provided the flexural strength and so only minimum longitudinal reinforcement was included to satisfy the requirements of the New Zealand Concrete Structures Standard (2006). Due to the high strains expected in the wall toe each wall panel had specifically designed confinement reinforcement in the corner regions of the precast wall. This consisted of 6 mm hoop stirrups spaced at 40 mm centers over the bottom 200 mm of the wall, with the spacing increased to 80 mm for a further 300 mm of wall height, as shown in Figure 2a. The confinement reinforcement was designed using the confined concrete model presented by Mander et al. (1988) using the maximum expected compressive strain calculated from the simplified analysis method developed by Aaleti et al. (2009). Two 40 mm drossbach ducts were cast into each wall to accommodate one 15 mm steel tendon each. The tendons had a measured yield strength of 900 MPa, an ultimate strength of 1100 MPa, and a modulus of elasticity of 215 GPa. A steel angle base frame constructed from 25×25×5 equal angle was cast into each precast wall end for additional confinement and protection of the edge, as shown in Figure 2b. The wall was seated on a foundation block designed with a 30 mm steel lined recess to enable grout to be removed easily following a test, allowing for the foundation to be reused for multiple tests, as shown in Figure 2c.

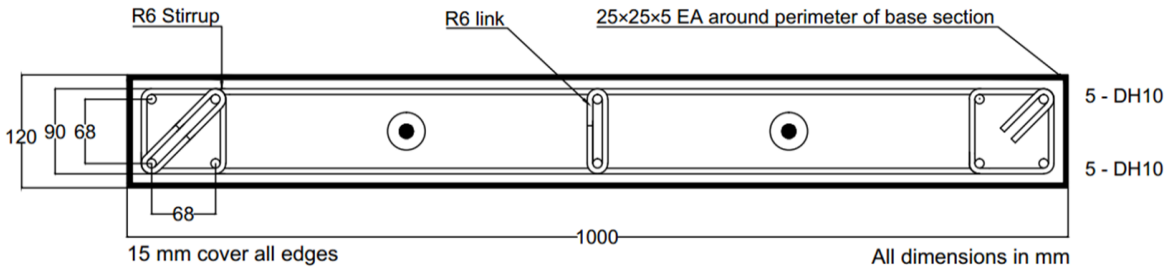

Figure 1. Cross-section of the precast concrete wall panel

(a) Confinement detail of wall end **(b)** Steel angle base frame **(c)** Foundation

Figure 2. Photos of the wall and foundation during construction

2.2. Test setup

A schematic of the test setup is shown in Figure 3a. The wall panel was seated on a foundation that was post-tensioned to a strong floor. A mass block was placed on top of the wall and post-tensioned tendons were anchored between the top of the mass block and the underside of the strong floor. Stability struts, which are shown in red in Figure 3b, were used to prop the wall during setup and ensure the wall remained vertical. While the wall was propped, grout was placed between the wall-to-foundation interface to provide an even bearing surface for the specimen. A high strength, high flow grout was used and purposely flowed from one side of the wall to the other to prevent the formation of air pockets. Following grouting a 1100 kg concrete mass block was attached to the top of the wall; this mass block served multiple purposes, including providing anchorage for the tendons, seismic mass for the dynamic testing, a loading beam for the actuator to be attached, and an anchorage/platform for

the Eccentric Mass Shaker (EMS) during forced vibration testing. For both the pseudo-static and high speed cyclic testing a ± 300 kN capacity hydraulic actuator was used to apply the cyclic lateral displacements to the top of the wall. The actuator was mounted to a strong wall 3.1 m above the wall-foundation interface and attached to the wall by means of the mass block. A lateral support frame provided out-of-plane restraint which prevented twisting and buckling of the wall during loading. A gap of 5 mm was left between the lateral support frame and the specimen during testing to allow small movements and to reduce the influence of friction on the sliding interface.

For the forced vibration testing the actuator was removed to allow the structure to be loaded by the EMS depicted in Figure 3b. For all tests the EMS remained in place to provide a consistent additional weight of 600 kg. Free vibration testing was undertaken using the setup shown in Figure 4. A quick release mechanism was secured to the wall, connected to a chain, 100 kN actuator and a load cell. The quick release shackle could be remotely triggered to release the wall from a specified lateral displacement.

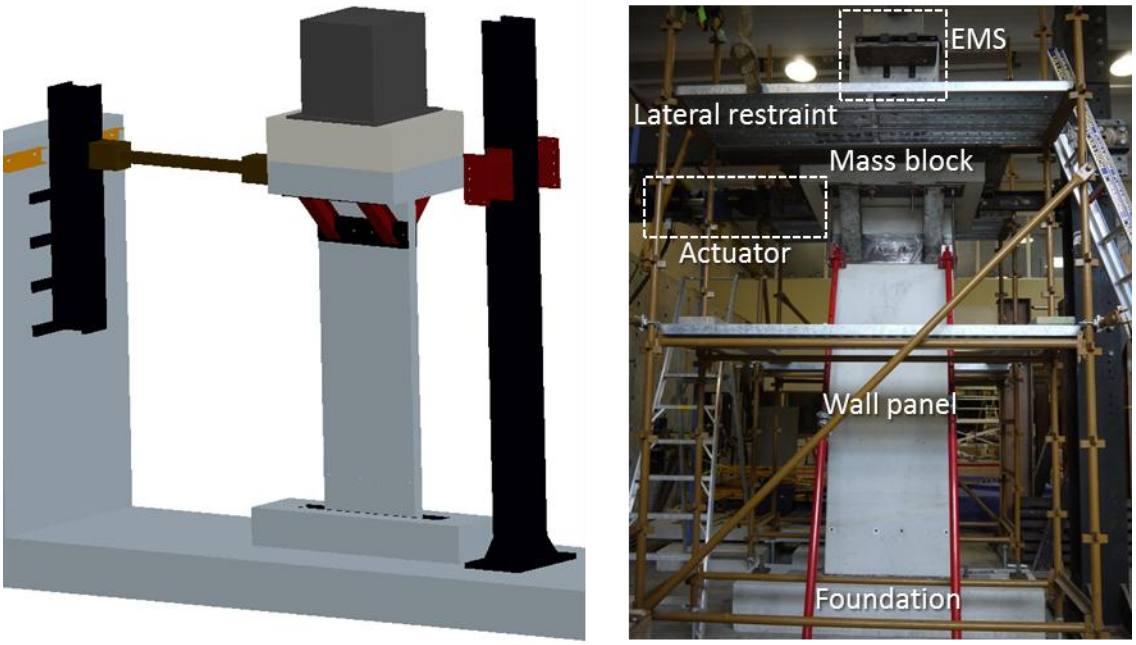

(a) Schematic **(b)** Photo

Figure 3. Test setup

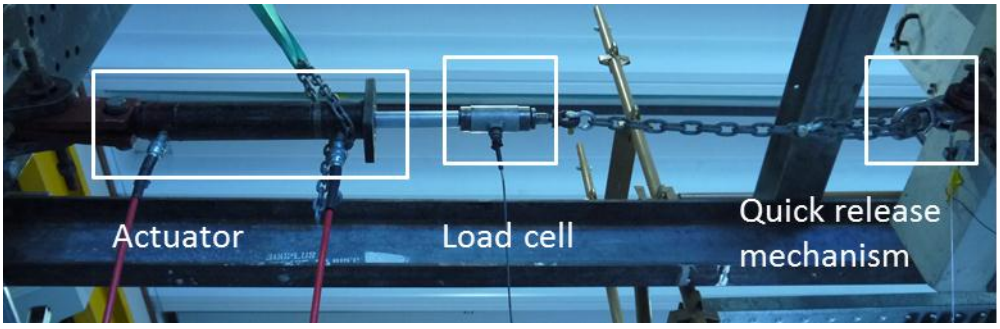

Figure 4. Setup for free vibration testing

2.3. Instrumentation

Extensive instrumentation was employed to monitor the behaviour of the wall during each of the tests. The instrumentation arrangement can be seen in Figure 5. For all four tests a Linear Variable Displacement Transducer (LVDT) and two string potentiometers (SP) were used to measure the in-

plane lateral displacement at the top of the wall. Portal Gauges (PG) were used to measure uplift at the wall-to-foundation interface, as well as slip at the wall-to-foundation, wall-to-mass block, and foundation-to-floor interfaces. Load Cells (LC) were used to measure the tendon force and the applied force to the specimen. During the cyclic loading the panel deformation was also measured using portal gauges. During the pseudo-static cyclic test the concrete compressive strains were measured at each wall corner using both Surface mounted Strain Gauges (SSG) and Internal Strain Gauges (ISG). For the dynamic testing accelerometers (A) were placed at the same height as the LVDT on both sides of the mass block and at each wall toe.

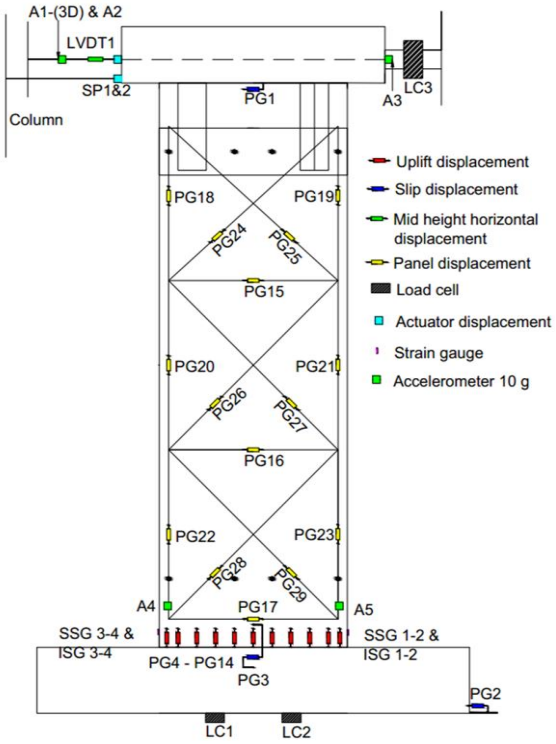

Figure 5. Typical instrumentation setup

2.4. Load protocol

2.4.1. Pseudo-static cyclic test and high speed cyclic test

The cyclic loading history based on ACI recommendations (2008) is shown in Figure 6a and was applied to the wall for both the pseudo-static and high speed cyclic tests. The wall was subjected to a maximum lateral drift of ±2% to limit damage and prevent the tendons from reaching yield. Three full reverse cycles were applied at each drift up to that level. For the pseudo-static test the loading history was applied at a rate of 0.5 mm/s. For the high-speed test the loading history was applied at a rate of 200 mm/s which resulted in a frequency range of 0-20 Hz.

2.4.2. Free vibration testing

The free vibration tests were conducted by applying a predetermined lateral displacement to the wall using the setup previously shown in Figure 4. At the desired drift the quick release mechanism was released and the wall was free to undergo a controlled rocking motion and decay. Free vibration testing was conducted for lateral drifts of 0.3%, 0.5%, 0.75%, 1% and 1.5%.

2.4.3. Forced vibration

An eccentric mass shaker (EMS) was used to excite the specimen into the rocking mode. The EMS consists of two eccentrically weighted flywheels that rotate in opposite directions at a desired frequency resulting in a steady-state sinusoidal in-plane force excitation. The force output can be adjusted by varying the amount of eccentric mass attached to each flywheel. For this test the

maximum of 128 kg was attached to each flywheel; resulting in the highest force at the lowest frequency. It was decided to increase the frequency at 1 Hz intervals. The frequency change during the test can be seen in Figure 6b along with the corresponding maximum force. The frequency was increased from 0-1 Hz and then 1-2 Hz achieving a steady-state response at each frequency. The frequency was then intended to be increased from 2-3 Hz but while increasing to 3 Hz the lateral displacement response of the structure increased substantially and the EMS was stopped so that the frequency decreased to zero.

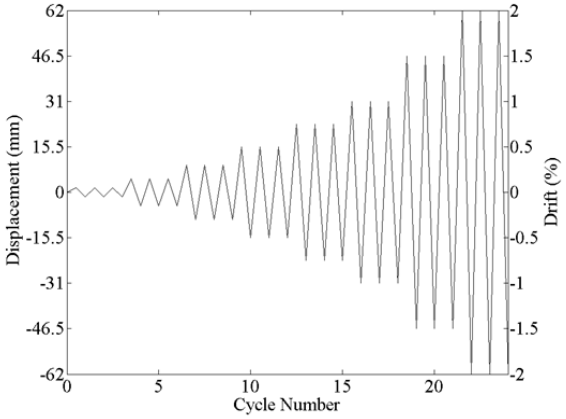

(a) Applied displacement history during cyclic tests

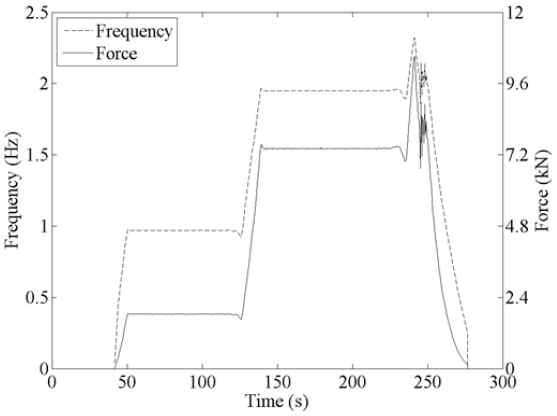

(b) Frequency and corresponding force loading history for the EMS excitation

Figure 6. Loading histories for the cyclic and EMS tests

3. RESULTS AND DISCUSSION

3.1. Pseudo-static cyclic test and high speed cyclic test

The measured lateral load response of the wall specimen subjected to pseudo-static cyclic loading is shown in Figure 7a and a photo of the wall uplift at 2% lateral drift is shown in Figure 7b. A comparison is made between the experimental response and the response calculated using a simplified analysis method developed by Aaleti and Sritharan (2009). It can be seen that the simplified analysis method predicted the wall response with reasonable accuracy. In Figure 8 the back bone of both the pseudo-static and high speed cyclic tests are presented showing a typical bilinear hysteresis. The high speed test resulted in a lower lateral force at higher drifts in comparison to the pseudo-static test.

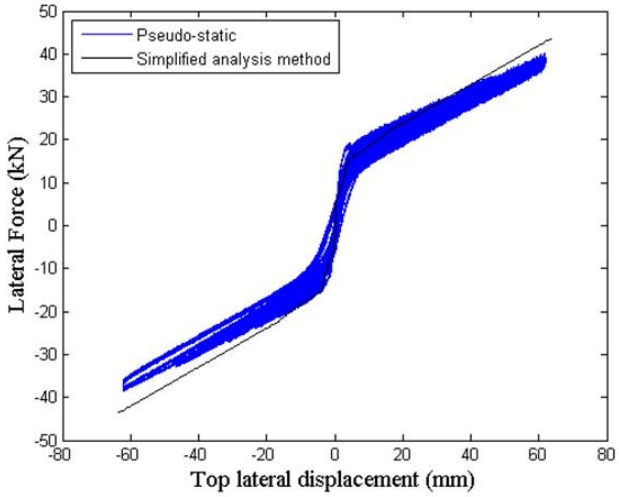

(a) Measured cyclic lateral load response

(b) Uplift at base

Figure 7. Results from the pseudo-static test

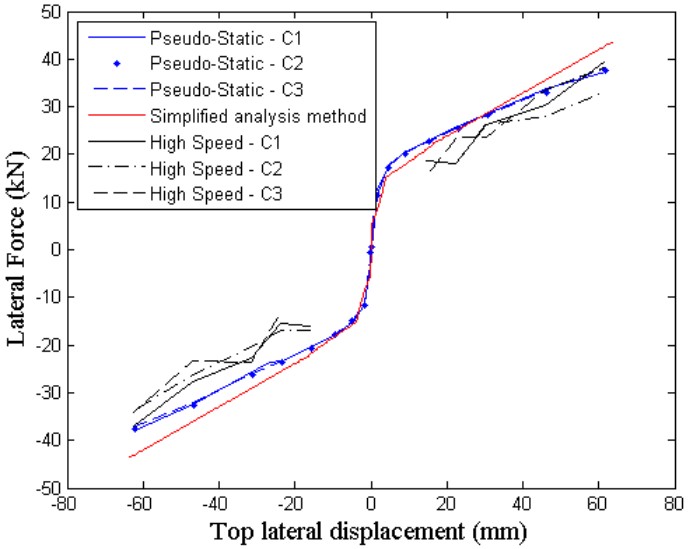

Figure 8. Backbone lateral load response of the specimen for pseudo-static and high speed cyclic loading

3.2. Free vibration

The free vibration test provides the opportunity to study the dynamic characteristics of the unbonded post-tensioned rocking wall system without any additional external excitation. The top lateral displacement, velocity and acceleration decay from the 1.0% drift test is shown in Figure 9. The displacement was directly measured with the LVDT and the velocity and acceleration were calculated numerically from the displacement measurement.

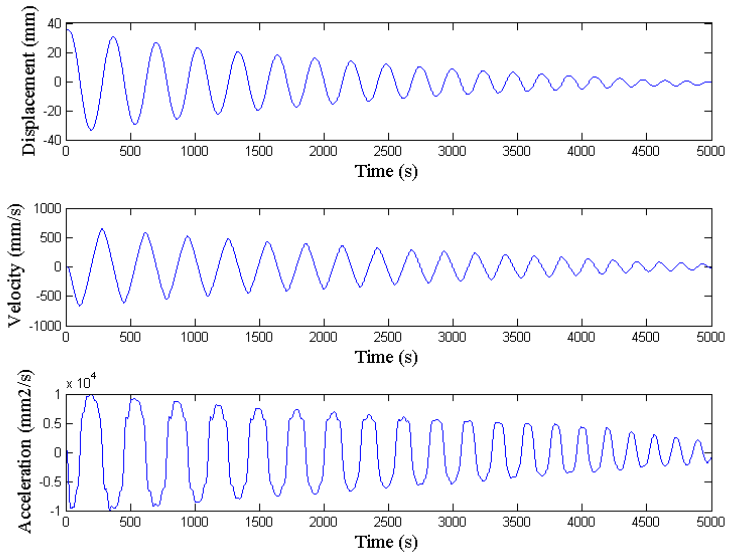

Figure 9. Free vibration decay from 1.0% lateral drift

The apparent Coefficients Of Restitution (COR) was calculated as described in section 1 by obtaining a ratio of the successive total energy content and plotted against the peak displacement preceding the impact at the Top of the Wall (ToW). The COR calculated using the Housner equation (eq. 1.1) is also plotted to compare the theoretical value with the experimental values. The experimental values show good alignment with the theoretical value from Housner's equation. The COR tended to be greater than the Housner value for negative displacement and less for the positive displacements. A possible reason for this trend is due imperfections in the placement of the post-tensioned tendons. Although Housner's COR equation was developed for a rigid rocking block it is also applicable for a post-

tensioned wall assuming the post-tensioned force only affects the system by increasing the gravity load.

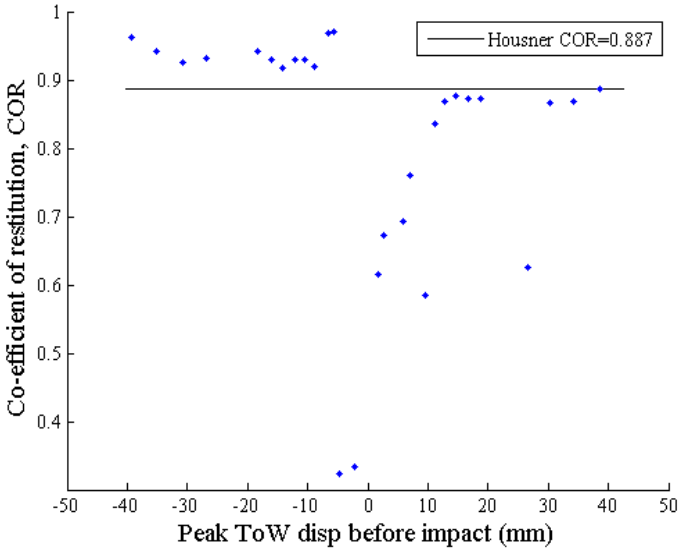

Figure 10. Apparent co-efficient of restitution for 1.5% drift

3.3. Forced vibration

The forced vibration testing using the EMS was undertaken to investigate the rocking response with change in frequency and force. The applied loading shown in Figure 6a produced the lateral displacement response presented in Figure 11 top left. Zoomed sections are also shown in Figure 11 for the 1 Hz, 2 Hz and 2-3 Hz response.

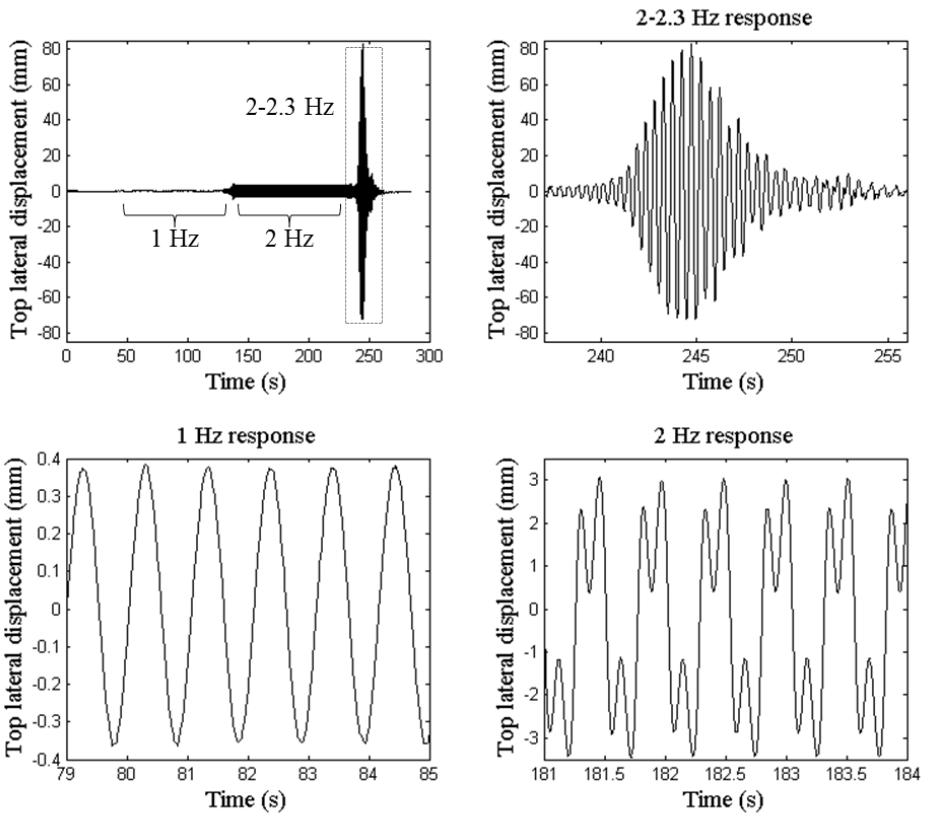

Figure 11. Top lateral displacement response to EMS

During the EMS test a low lateral displacement amplitude of seemingly steady-state rocking motion was observed for both the 1 Hz and 2 Hz excitation frequencies. Table 3.3.1 shows the maximum expected lateral displacement and drift for the maximum moment applied by the EMS using Aaleti and Sritharan's Simplified Analysis Method (SAM) which is based on a static force calculation. The maximum measured displacement and drift for the corresponding moment is also presented in Table 3.3.1, this shows the difference between a static analytical prediction and the measured dynamic response. The moment is calculated based on the frequency of the shaker converted into a force, then multiplied by the leverarm of 3.8 m (distance from base of wall to the centre of the rotating flywheels). The amplitude of excitation at 1 and 2 Hz was close to what you would expect based on SAM although slightly larger during the test which is not surprising given that the excitation is dynamic and not static. As the frequency of the EMS was ramped from 2-3 Hz a large increase in displacement was observed which does not align with expected values using SAM. As shown in Figure 11 this lateral displacement response did not appear to be entering a steady-state motion but continued to increase until the EMS was stopped. The point when the amplitude of displacement stops increasing is when the EMS was shut down. A possible explanation for this large increase in displacement is due to the harmonic nature of the EMS loading. Controlled rocking systems under a predictable harmonic loading have been shown analytically to have unpredictable response and can exhibit classical chaotic rocking system traits (Ma, 2010).

Table 3.3.1 EMS response results

Frequency (Hz)	Moment(kNm)	Umax (mm)		Drift (%)	
		Experimental	SAM*	Experimental	SAM*
1	6.9	0.4	<0.27	0.01	0.009
2	28.2	3.0	2	0.10	0.065
2.3	40.0	82.9	3	2.67	0.1

*SAM - Simplified Analysis Method (Aaleti, 2009)

4. CONCLUSIONS AND FUTURE RESEARCH

An unbonded post-tensioned rocking wall was subjected to four different loading conditions to investigate the cyclic and dynamic response. A single rocking wall panel was subjected to pseudo-static cyclic loading, high speed cyclic loading, free vibration decay and forced vibration. The comparison of lateral force response of the high speed and pseudo static cyclic tests showed that with the introduction of velocity a reduced force was observed at higher drifts. The free vibration decay was used to determine the apparent coefficient of restitution for the system. This showed reasonable correlation with Hounser's co-efficient of restitution formula. An EMS was used to excite the wall into the rocking mode and the response in terms of lateral displacement was presented. When the EMS reached a certain frequency the displacement response increased substantially. The increase in lateral displacement did not correlate with the increase in force.

The EMS testing, free vibration testing and the fast-cyclic testing presented here will be conducted again on an identical wall to investigate the undamaged response of each of the loadings. Following the completion of the single precast panel testing phase the same test plan will be performed on a specimen with additional energy dissipating devices to investigate the interaction of hysteretic and contact damping on the overall dynamic response. In situ testing is then expected to be carried out on both wall specimens to consider the effect of real soil conditions on the dynamic response of the systems using both forced vibration testing and free vibration testing.

ACKNOWLEDGEMENT
The authors would like to acknowledge the support and materials donated by Stresscrete (Papakura) and Mapei. Additionally the assistance of Dan Ripley, Jeffrey Ang, Mark Byrami, and Sam Corney during the experimental programme is greatly appreciated.

REFERENCES

AALETI, S. & SRITHARAN, S. 2009. A simplified analysis method for characterizing unbonded post-tensioned precast wall systems. *Engineering Structures,* 31**,** 2966-2975.

ACI INNOVATION TASK GROUP 5. 2008. *Acceptance criteria for special unbonded post-tensioned precast structural walls based on validation testing and commentary : an ACI standard,* Farmington Hills, Mich., American Concrete Institute.

CHENG, C. T. 2007. Energy dissipation in rocking bridge piers under free vibration tests. *Earthquake Engineering and Structural Dynamics,* 36**,** 503-518.

CHENG, C. T. 2008. Shaking table tests of a self-centering designed bridge substructure. *Engineering Structures,* 30**,** 3426-3433.

ERKMEN, B. & SCHULTZ, A. E. 2009. Self-centering behavior of unbonded, post-tensioned precast concrete shear walls. *Journal of Earthquake Engineering,* 13**,** 1047-1064.

HENRY, R. S., AALETI, S., SRITHARAN, S. & INGHAM, J. M. 2010. Concept and finite-element modeling of new steel shear connectors for self-centering wall Systems. *Journal of Engineering Mechanics,* 136**,** 220-229.

HENRY, R. S., BROOKE, N. J., SRITHARAN, S. & INGHAM, J. M. 2012. Defining concrete compressive strain in unbonded post-tensioned walls. *ACI Structural Journal,* 109**,** 101-112.

HOLDEN, T., RESTREPO, J. & MANDER, J. B. 2003. Seismic performance of precast reinforced and prestressed concrete walls. *Journal of Structural Engineering,* 129**,** 286-296.

HOUSNER, G. W. 1963. The behavior of inverted pendulum structures during earthquakes. *Bulletin of the Seismological Society of America,* 53**,** 403-417.

KURAMA, Y., PESSIKI, S., SAUSE, R. & LU, L. W. 1999a. Seismic behavior and design of unbonded post-tensioned precast concrete walls. *PCI Journal,* 44**,** 72-89.

KURAMA, Y., SAUSE, R., PESSIKI, S. & LU, L. W. 1999b. Lateral load behavior and seismic design of unbonded post-tensioned precast concrete walls. *ACI Structural Journal,* 96**,** 622-632.

KURAMA, Y. C. 2000. Seismic design of unbonded post-tensioned precast concrete walls with supplemental viscous damping. *ACI Structural Journal,* 97**,** 648-658.

KURAMA, Y. C., SAUSE, R., PESSIKI, S. & LU, L. W. 2002. Seismic response evaluation of unbonded post-tensioned precast walls. *ACI Structural Journal,* 99**,** 641-651.

MA, Q. T. M. 2010. *The mechanics of rocking structures subjected to ground motion.* PhD--Civil and Environmental Engineering, University of Auckland.

MANDER, J. B., PRIESTLEY, M. J. N. & PARK, R. 1988. THEORETICAL STRESS-STRAIN MODEL FOR CONFINED CONCRETE. *Journal of structural engineering New York, N.Y.,* 114**,** 1804-1826.

MARRIOTT, D., PAMPANIN, S., BULL, D. & PALERMO, A. 2008. Dynamic testing of precast, post-tensioned rocking wall systems with alternative dissipating solutions. *Bulletin of the New Zealand Society for Earthquake Engineering,* 41**,** 90-103.

NAKAKI, S. D., STANTON, J. F. & SRITHARAN, S. 1999. Overview of the PRESSS five-story precast test building. *PCI Journal,* 44**,** 26-39.

NEW ZEALAND STANDARD 2006. Concrete Structures Standard NZS 3101.

PEREZ, F. J., PESSIKI, S. & SAUSE, R. 2004. Lateral load-behavior of unbonded post-tensioned precast concrete walls with vertical joints. *PCI Journal,* 49**,** 48-+.

PEREZ, F. J., PESSIKI, S., SAUSE, R. & LU, L. M. 2003. Lateral load tests of unbonded post-tensioned precast concrete walls. *In:* ISSA, M. A. & MO, Y. L. (eds.) *Large-Scale Structural Testing.* Farmington Hills: American Concrete Institute.

PRIESTLEY, M. J. N. 1991. Overview of PRESSS research program. *PCI Journal,* 36**,** 50-57.

PRIESTLEY, M. J. N., SRITHARAN, S. S., CONLEY, J. R. & PAMPANIN, S. 1999. Preliminary results and conclusions from the PRESSS five-story precast concrete test building. *PCI Journal,* 44**,** 42-67.

RESTREPO, J. I. & RAHMAN, A. 2007. Seismic performance of self-centering structural walls incorporating energy dissipators. *Journal of Structural Engineering,* 133**,** 1560-1570.

SRITHARAN, S., AALETI, S. & THOMAS, D. J. 2007. Seismic analysis and design of precast concrete jointed wall systems. *ISU-ERI-Ames Report ERI-07404.* Ames, IA: Department of Civil, Construction and Environmental Engineering, Iowa State University.

WIGHT, G. D., INGHAM, J. M. & KOWALSKY, M. J. 2006. Shaketable testing of rectangular post-tensioned concrete masonry walls. *ACI Structural Journal,* 103**,** 587-595.

WIGHT, G. D., KOWALSKY, M. J. & INGHAM, J. M. 2007. Shake table testing of posttensioned concrete masonry walls with openings. *Journal of Structural Engineering,* 133**,** 1551-1559.